Clim Dyn
DOI 10.1007/s00382-016-3361-7

Projection of future changes in the frequency of intense tropical cyclones

Masato Sugi[1] · **Hiroyuki Murakami**[1,2] · **Kohei Yoshida**[1]

Received: 3 June 2016 / Accepted: 11 September 2016

Abstract Recent modeling studies have consistently shown that the global frequency of tropical cyclones will decrease but that of very intense tropical cyclones may increase in the future warmer climate. It has been noted, however, that the uncertainty in the projected changes in the frequency of very intense tropical cyclones, particularly the changes in the regional frequency, is very large. Here we present a projection of the changes in the frequency of intense tropical cyclones estimated by a statistical downscaling of ensemble of many high-resolution global model experiments. The results indicate that the changes in the frequency of very intense (category 4 and 5) tropical cyclones are not uniform on the globe. The frequency will increase in most regions but decrease in the south western part of Northwest Pacific, the South Pacific, and eastern part of the South Indian Ocean.

Keywords Intense tropical cyclones · Climate change · Ensemble high-resolution global models · Statistical downscaling · Intensity bias correction

✉ Masato Sugi
msugi@mri-jma.go.jp

[1] Meteorological Research Institute, 1-1 Nagamine, Tsukuba, Ibaraki, Japan

[2] Geophysical Fluid Dynamics Laboratory, Princeton, NJ, USA

1 Introduction

Knutson et al. (2010) concluded that existing modeling studies consistently project decreases in the globally averaged frequency of tropical cyclones, and higher resolution modeling studies typically project substantial increases in the frequency of the most intense cyclones. Recently the confidence of these conclusions is further enhanced by many additional high-resolution model experiments (IPCC 2013; Murakami et al. 2015; Roberts et al. 2015; Wehner et al. 2015; Walsh et al. 2016). However, it is noted that there remains a very large uncertainty in the projected changes in the very intense tropical cyclone frequency, particularly in the regional frequency (Figure 14.17 of IPCC 2013). The uncertainty is so large that it is difficult to draw any useful information for risk assessment. The main reason for the very large uncertainty is a lack of many high resolution global models that realistically simulate very intense (category 4 and 5) tropical cyclones.

To make a more reliable estimation of the changes in very intense tropical cyclone frequency, Knutson et al. (2013, 2015) employed a dynamical downscaling method. Knutson et al. (2015) downscaled all the tropical storms simulated by the higher resolution global atmospheric model (GFDL HiRAM; 50 km grid) by using the GFDL hurricane model (nested grid model; 6 km grid near the storm). Their results indicate that the frequency of very intense tropical cyclones will increase in most ocean basins but it will decrease in the South Pacific, the eastern Indian Ocean and southern section of the Northwest Pacific. The results of Knutson et al. (2015) seem to be considerably more reliable than IPCC (2013). However, their results are based on a single 20 year (tropical cyclone season) global model simulation, and the number

Published online: 29 September 2016

of simulated very intense tropical cyclones is still insufficient to make a statistically reliable estimation of the change.

In the present study, we estimate the changes in intense tropical cyclone frequency based on a statistical downscaling of ensemble of many high-resolution global model experiments. In Sect. 2, the experiment data and the statistical downscale method are described. The main results are presented in Sect. 3, followed by discussions in Sect. 4 and conclusions in Sect. 5.

Table 1 List of experiments

ID	PD/GW	Experiment	AGCM version	Resolution (km)	Convection scheme	SST/SSTA
P1	PD	HP0A	3.1	60	AS	HadISST
P2	PD	HP0A_m01	3.1	60	AS	HadISST
P3	PD	HP0A_m02	3.1	60	AS	HadISST
P4	PD	HPA_m00	3.2	60	YS	HadISST
P5	PD	HPA_m01	3.2	60	YS	HadISST
P6	PD	HPA_m02	3.2	60	YS	HadISST
P7	PD	HPA	3.2	60	YS	HadISST
P8	PD	HPA_kf	3.2	60	KF	HadISST
P9	PD	HPA_as	3.2	60	AS	HadISST
P10	PD	SP0A	3.1	20	AS	HadISST
P11	PD	SPA	3.2	20	YS	HadISST
F1	GW	HF0A	3.1	60	AS	CMIP3 ensemble mean
F2	GW	HF0A_m01	3.1	60	AS	CMIP3 ensemble mean
F3	GW	HF0A_m02	3.1	60	AS	CMIP3 ensemble mean
F4	GW	HF0A_csiro	3.1	60	AS	CMIP3 CSIRO
F5	GW	HF0A_csiro_m01	3.1	60	AS	CMIP3 CSIRO
F6	GW	HF0A_csiro_m02	3.1	60	AS	CMIP3 CSIRO
F7	GW	HF0A_miroc	3.1	60	AS	CMIP3 MIROC_high
F8	GW	HF0A_miroc_m01	3.1	60	AS	CMIP3 MIROC_high
F9	GW	HF0A_miroc_m02	3.1	60	AS	CMIP3 MIROC_high
F10	GW	HF0A_mri	3.1	60	AS	CMIP3 MRI
F11	GW	HF0A_mri_m01	3.1	60	AS	CMIP3 MRI
F12	GW	HF0A_mri_m02	3.1	60	AS	CMIP3 MRI
F13	GW	HFA_m00	3.2	60	YS	CMIP3 ensemble mean
F14	GW	HFA_m01	3.2	60	YS	CMIP3 ensemble mean
F15	GW	HFA_m02	3.2	60	YS	CMIP3 ensemble mean
F16	GW	HFA	3.2	60	YS	CMIP3 ensemble mean
F17	GW	HFA_cluster1	3.2	60	YS	CMIP3 cluster1
F18	GW	HFA_cluster2	3.2	60	YS	CMIP3 cluster2
F19	GW	HFA_cluster3	3.2	60	YS	CMIP3 cluster3
F20	GW	HFA_kf	3.2	60	KF	CMIP3 ensemble mean
F21	GW	HFA_kf_cluster1	3.2	60	KF	CMIP3 cluster1
F22	GW	HFA_kf_cluster2	3.2	60	KF	CMIP3 cluster2
F23	GW	HFA_kf_cluster3	3.2	60	KF	CMIP3 cluster3
F24	GW	HFA_as	3.2	60	AS	CMIP3 ensemble mean
F25	GW	HFA_as_cluster1	3.2	60	AS	CMIP3 cluster1
F26	GW	HFA_as_cluster2	3.2	60	AS	CMIP3 cluster2
F27	GW	HFA_as_cluster3	3.2	60	AS	CMIP3 cluster3
F28	GW	SF0A	3.1	20	AS	CMIP3 ensemble mean
F29	GW	SFA	3.2	20	YS	CMIP3 ensemble mean

P1–P11 indicates present day (PD) climate simulations, and F1–F29 indicates future global warming (GW) climate simulations. Convection schemes are AS (Arakawa-Shubert scheme, Arakawa and Schubert 1974; Randall and Pan 1993), YS (Yoshimura scheme, Yoshimura et al. 2015) and KF (Kain-Fritch scheme, Kain and Fritsch 1990, 1993)

2 Data and method

We used simulation data from an ensemble of many high resolution global model experiments conducted at Meteorological Research Institute (MRI) (Murakami et al. 2012a, b; Sugi and Yoshimura 2012). These experiments are listed in Table 1. The experiments are 25 year simulations of the present day (PD) climate (11 members) and the future global warming (GW) climate (29 members). Models used for the experiments are various versions of MRI-AGCM3, with horizontal resolution 60 km and 20 km, and with three different convection schemes. The sea surface temperature (SST) for the PD experiments (1979–2003) is the observed SST (HadISST1; Rayner et al. 2003). For the GW experiments (2075–2099), seasonally varying average SST change estimated by the 18 member ensemble of Coupled Model Intercomparison Project phase 3 (CMIP3) models is added to the PD experiment SST (see Murakami et al. 2012a for the further detail). The atmospheric concentration of greenhouse gases and aerosols in the experiments is based on the Intergovernmental Panel on Climate Change (IPCC) A1B scenarios.

Among the 40 experiments listed in Table 1, the only two experiments (P11 and F29) using the 20 km grid AGCM3.2 could simulate very intense tropical cyclones realistically. In all the other experiments, the intensity of simulated tropical cyclones is generally much weaker than that of observed tropical cyclones and very intense tropical cyclones are not simulated. To estimate the possible future changes in the frequency of very intense tropical cyclones using these experiments, some downscaling method is needed for these experiments. Here we employ a statistical downscaling method, in which the intensity bias of the simulated tropical cyclones is corrected by a statistical method. The basic idea of the statistical downscaling is that the most intense (e.g. top 20 %) simulated tropical cyclones correspond to the most intense observed tropical cyclones, and the response to a climate forcing of the most intense observed tropical cyclones should be represented by that of the most intense simulated tropical cyclones. In this argument, we assume that the bias (the difference between the intensities of simulated and observed tropical cyclones) is the same for PD simulations and GW simulations. We believe that this is a reasonable assumption, because the changes between PD and GW simulations are not so large.

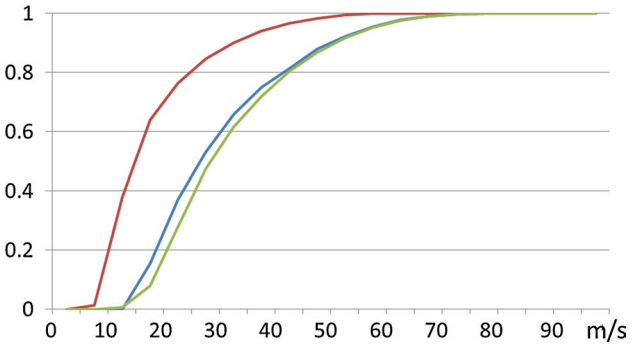

Fig. 1 Intensity bias correction based on cumulative distribution function (CDF). This figure illustrates the bias correction for the PD simulation (P7 experiment). *Red*, *blue* and *green curves* indicate the simulated, adjusted and observed CDF, respectively

The statistical method of bias correction is similar to the method used by Zhao and Held (2010). As shown in Fig. 1, we use a cumulative distribution function (CDF). The wind speed of a simulated tropical cyclone is adjusted to the wind speed of the observed tropical cyclone with the same probability in the CDF. We applied the statistical bias correction for each 5° latitude band in each ocean basin. This is because the intensity biases are not the same everywhere. As the model tends to develop tropical cyclones slowly compared to the observation, the intensity of simulated tropical cyclones tends to be weaker in the low latitudes and stronger in the high latitudes. This bias has been noted as a northward bias of intense tropical cyclones in the northern hemisphere (Murakami et al. 2012a). By applying the bias correction to each latitude band, such a northward bias is also reduced. Figure 2 shows the observed, simulated and adjusted tropical cyclone tracks with intensity indicated by different colors. The intensity of simulated tropical cyclones in the experiment P10 using a 60 km grid model (Fig. 2b) is generally much weaker than that of observed tropical cyclones (Fig. 2a), while the intensity of the adjusted tropical cyclones (Fig. 2c) is close to that of observed tropical cyclones.

As observation data of tropical cyclone climatology, we used dataset available on Unisys corporation website (2012) which consists of best-track TC data compiled by the National Hurricane Center (NHC) and Joint Typhoon Warning Center (JTWC).

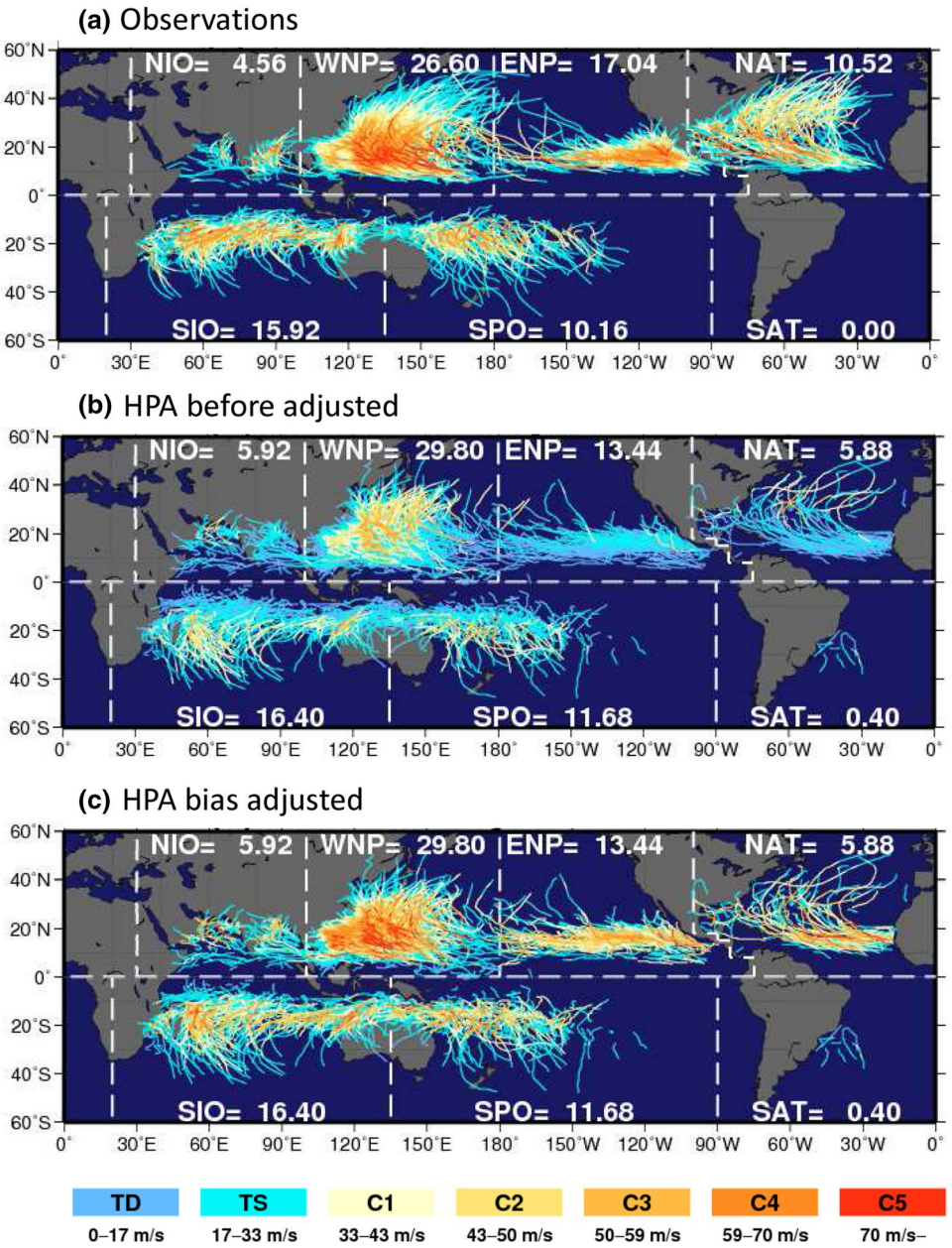

Fig. 2 Tropical cyclone tracks with intensity shown by *colors*. **a** Observed, **b** simulated by 60 km resolution model experiment (P7), **c** adjusted by the intensity bias correction

3 Results

We examine the changes in tropical cyclone number (TC number) and tropical cyclone days (TC days) in various intensity categories: all tropical storms (cat 0–5; $V_{max} \geq 17$ m/s), hurricanes (cat 1–5; $V_{max} \geq 33$ m/s), major hurricanes (cat 3–5; $V_{max} \geq 50$ m/s) and very intense tropical cyclones (cat 4–5; $V_{max} \geq 59$ m/s). For the TC number, the intensity category is defined by the lifetime maximum wind speed for each tropical cyclone. For the TC days, the intensity category is defined by the maximum wind speed of a tropical cyclone every 6 h, and the duration (number of days) of the tropical cyclone staying in each category is calculated.

Table 2 Tropical cyclone numbers and their changes in various intensity categories for global domain and by ocean basin

	Global	North Indian	Northwest Pacific	Northeast Pacific	North Atlantic	South Indian	South Pacific
TC number cat 0–5							
OBS	84.8	4.8	26.5	17.1	10.4	16.3	9.8
P	84.0	6.1	22.7	19.2	6.2	18.3	11.6
F	66.6	5.5	17.6	14.7	5.0	15.5	8.4
F − P	**−17.4**	−0.6	**−5.1**	−4.5	**−1.2**	**−2.8**	**−3.3**
(F − P)/P (%)	**−20.7**	−10.1	**−22.5**	−23.5	**−19.2**	**−15.0**	**−27.9**
p value	**0.00**	0.21	**0.04**	0.19	**0.02**	**0.00**	**0.00**
TC number cat 1–5							
OBS	47.8	1.6	17.0	9.7	5.8	8.6	5.1
P	55.6	3.0	15.6	15.5	4.3	10.7	6.6
F	48.4	3.1	13.5	12.2	3.8	10.7	5.2
F − P	**−7.2**	0.1	−2.1	−3.3	−0.5	0.0	**−1.4**
(F − P)/P (%)	**−12.9**	4.4	−13.3	−21.5	−12.4	0.4	**−21.5**
p value	**0.06**	0.61	0.17	0.32	0.12	0.98	**0.02**
TC number cat 3–5							
OBS	22.8	0.6	8.8	4.8	2.1	4.2	2.2
P	26.0	1.1	8.0	7.6	2.0	4.8	2.5
F	24.5	1.4	7.6	6.5	2.0	5.0	2.0
F − P	−1.5	0.2	−0.4	−1.2	0.1	0.2	**−0.5**
(F − P)/P (%)	−5.8	21.1	−4.6	−15.2	3.6	3.9	**−18.9**
p value	0.84	1.00	0.33	0.87	0.75	0.68	**0.08**
TC number cat 4–5							
OBS	14.4	0.4	6.2	3.2	1.2	2.4	1.0
P	12.1	0.5	4.9	2.3	1.1	2.2	1.0
F	12.0	0.6	4.7	2.2	1.3	2.4	0.8
F − P	−0.1	0.1	−0.2	−0.1	0.1	0.2	−0.2
(F − P)/P (%)	−0.7	21.2	−3.9	−4.4	12.4	8.2	−20.2
p value	0.87	0.82	0.64	0.63	0.86	0.70	0.11

P and F indicate ensemble average of the present day (PD) experiments and the future GW experiments, respectively. The *p* values are calculated using two-sided Mann–Whitney–Wilcoxon test. Bold letters indicate that the changes are statistically significant at 90 % significance level (*p* value is less than 0.1)

Table 2 summarizes the statistics of TC numbers in various intensity categories for global domain and by ocean basins. The model simulation data denoted by P and F are the ensemble mean of 11 member PD experiments (P1–P11) and 29 member GW experiments (F1-F29), respectively. These experiments are different from each other by resolution (20 or 60 km), SST anomaly for the GW experiments, convection schemes [Arakawa-Shubert scheme (AS), Yoshimura scheme (YS) or Kain-Fritch scheme (KF)] and initial conditions. All the simulation data are adjusted by the intensity bias correction as described in the previous section.

The average global tropical cyclone number simulated by PD experiments in each category is comparable to observation, with a little overestimation for cat 1–5 and cat 3–5, and underestimation for cat 4–5. The global number of all tropical storms (cat 0–5) significantly (21 %) decreases in the future warmer climate, while the more intense tropical cyclones show smaller decreases, with little (0.7 %) decreases in very intense tropical cyclones (cat 4–5). The

Table 3 Same as Table 2 but for occurrence frequency (TC days) in various intensity categories for global domain and by ocean basin

	Global	North Indian	Northwest Pacific	Northeast Pacific	North Atlantic	South Indian	South Pacific
tcdays cat 0–5							
OBS	419.5	13.8	149.8	76.5	52.5	80.9	46.2
P	361.3	19.4	103.9	74.2	27.5	87.2	49.1
F	281.3	17.9	76.2	57.7	22.0	74.7	32.8
F − P	**−80.0**	−1.6	**−27.7**	−16.5	**−5.5**	**−12.5**	**−16.3**
(F − P)/P(%)	**−22.1**	−8.0	**−26.7**	−22.2	**−19.9**	**−14.3**	**−33.2**
p value	**0.00**	0.33	**0.02**	0.22	**0.06**	**0.02**	**0.00**
tcdays cat 1–5							
OBS	173.6	2.9	71.3	32.2	23.0	29.0	15.2
P	175.8	5.6	56.0	43.6	14.3	36.2	20.1
F	157.0	6.9	47.9	36.0	13.1	38.7	14.5
F − P	−18.8	1.3	−8.2	−7.7	−1.1	2.5	**−5.5**
(F − P)/P(%)	−10.7	22.6	−14.6	−17.6	−8.0	6.8	**−27.5**
p value	0.09	0.91	0.11	0.41	0.25	0.73	**0.01**
tcdays cat 3–5							
OBS	51.1	0.8	23.7	9.3	5.1	8.2	3.8
P	59.7	1.8	21.2	15.2	4.8	11.2	5.6
F	61.2	2.6	21.4	13.9	5.3	13.8	4.3
F − P	1.5	0.8	0.1	−1.4	0.5	2.6	**−1.3**
(F − P)/P(%)	2.5	48.0	0.7	−8.9	10.7	23.3	**−22.5**
p value	0.87	0.52	0.54	0.86	0.70	0.16	**0.02**
tcdays cat 4–5							
OBS	26.6	0.4	14.2	4.1	2.6	3.8	1.6
P	21.8	0.5	10.3	3.4	2.1	3.5	1.9
F	25.0	0.9	11.5	3.6	2.6	4.9	1.6
F − P	3.3	0.4	1.1	0.2	0.5	**1.4**	−0.3
(F − P)/P(%)	15.0	68.5	10.9	6.2	21.3	**39.1**	−15.7
p value	0.30	0.48	0.79	0.82	0.66	**0.04**	0.13

number of all tropical storms (cat 0–5) in each ocean basin significantly (10–28 %) decreases, although the changes are not statistically significant for North Indian Ocean and Northeast Pacific Ocean. The changes in the number of tropical cyclones in more intense categories by ocean basins are not generally statistically significant, although the fractional changes in some ocean basins are large. The global changes (F−P) in cat 1–5 and cat 3–5 are contributed by Northeast Pacific Ocean. The small global change in the number of very intense tropical cyclones (cat 4–5) results from a mixture of increase and decrease in various ocean basins.

The similar statistics for TC days is shown in Table 3. The simulated global TC days in cat 0–5 are underestimated, indicating that the average lifetime of simulated tropical cyclones (4.4 days) is shorter than that of observation (4.9 days). The TC days of simulated tropical cyclone in more intense categories are generally comparable to observation, with somewhat overestimation in cat 3–5 and underestimation in cat 4–5. The TC days in cat 0–5 significantly (8–33 %) decrease globally and in each ocean basins, although the changes in the North Indian Ocean and the Northeastern Pacific Ocean are not statistically significant. The TC days in cat 1–5 decrease globally and in most ocean basins, while they increase in the Indian Ocean. These changes are not statistically significant except for the South Pacific Ocean. The TC days in more intense categories (cat 3–5 and cat 4–5) increase globally and in most ocean basins except for the South Pacific Ocean. These changes, however, are also not statistically significant except for the South Pacific Ocean.

Fig. 3 Occurrence frequency (TC days) of very intense tropical cyclones. **a** Observation, **b** ensemble mean of all the adjusted PD simulations (P1–P11), **c** Ensemble mean of all the adjusted GW simulations (F1–F29), and **d** the difference between GW and PD simulations [(**c**) minus (**b**)]. Unit is number of days per decade in 5° × 5° grid box

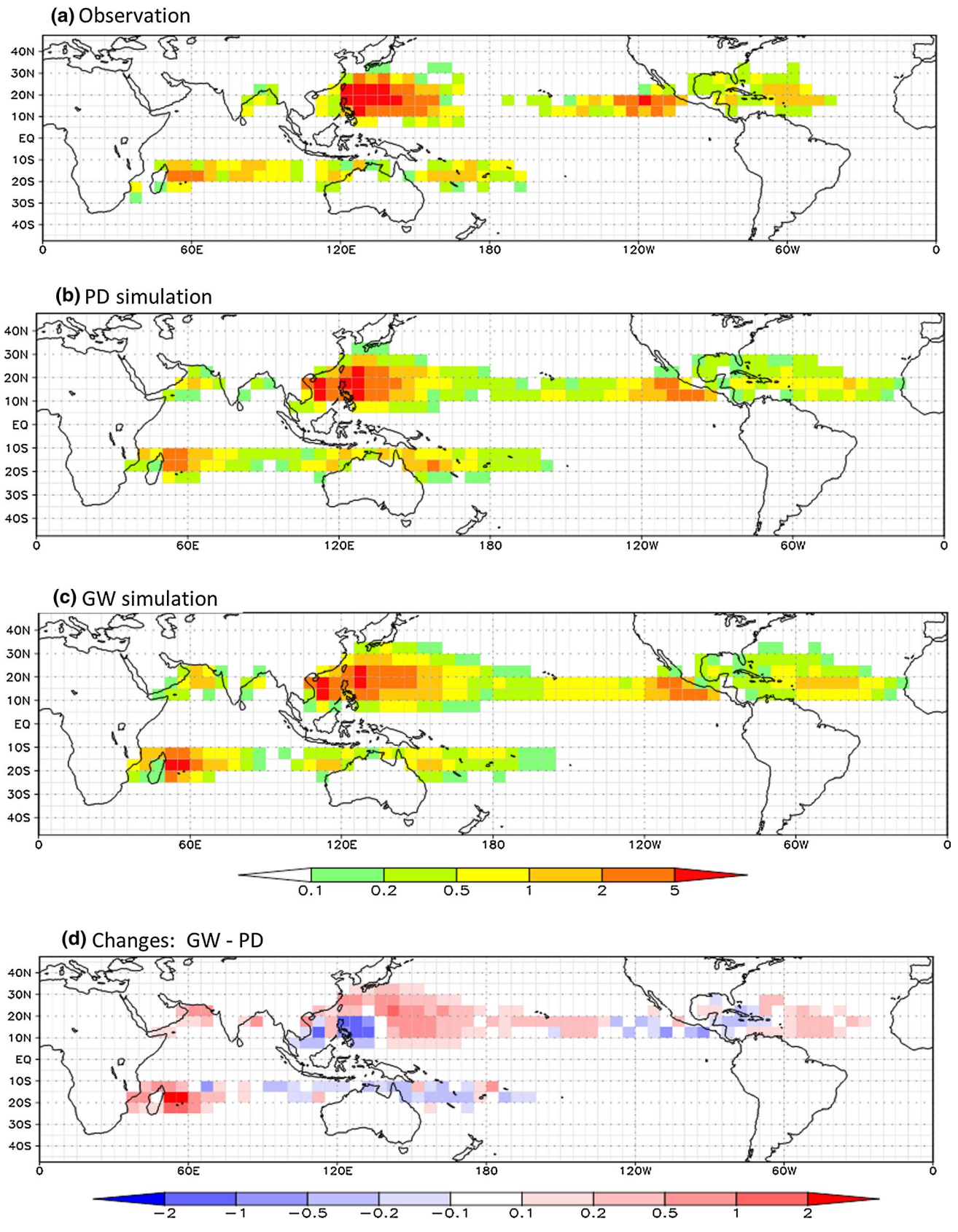
(a) Observation
(b) PD simulation
(c) GW simulation
(d) Changes: GW - PD
40N
30N
20N
10N
EQ
10S
20S
30S
40S
0
60E
120E
180
120W
60W
0.1
0.2
0.5
1
2
5
−2
−1
−0.5
−0.2
−0.1
0.1
0.2
0.5
1
2

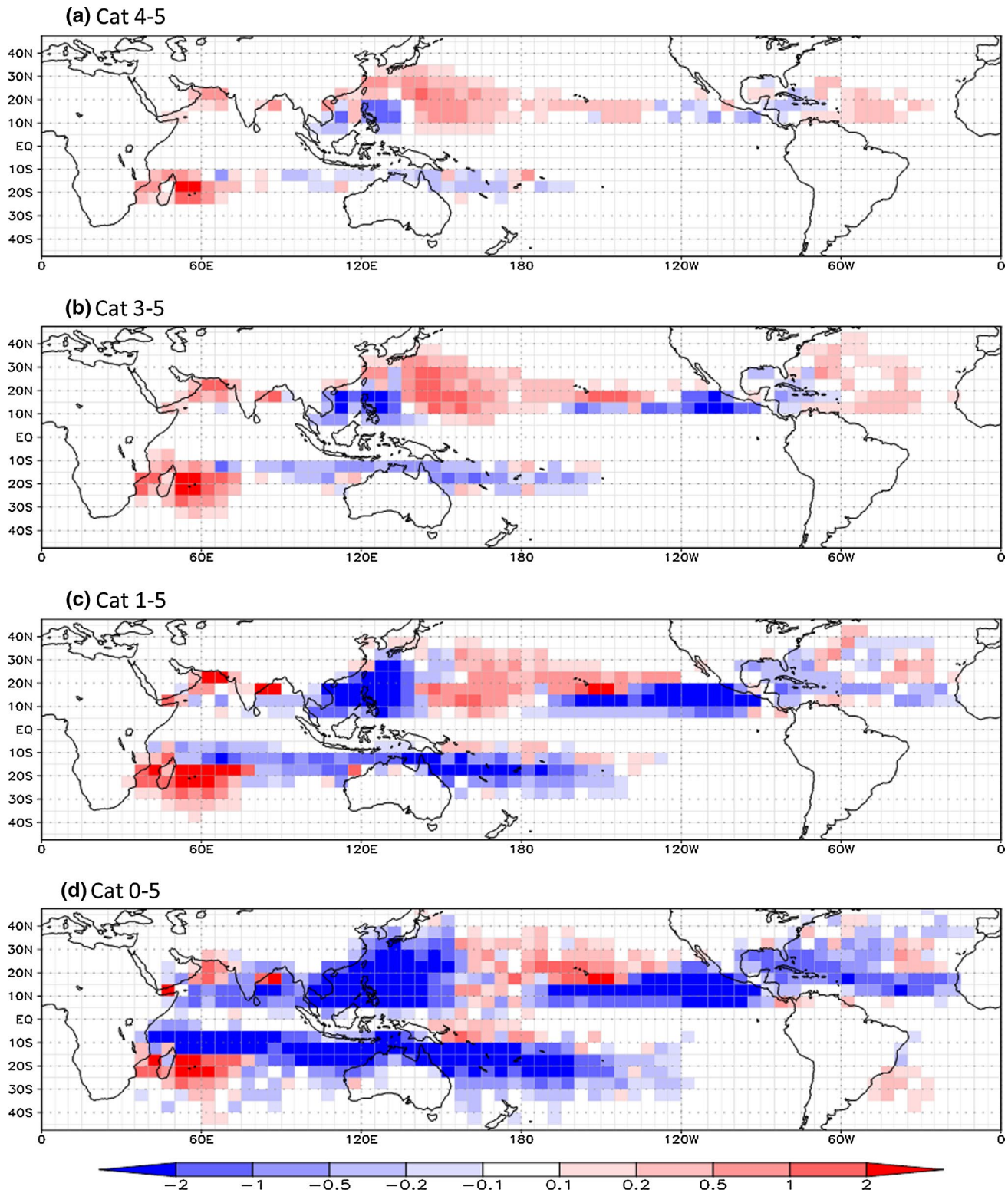

Fig. 4 Changes in occurrence frequency (TC days) of tropical cyclones in various intensity categories. **a** All tropical storms (cat 0–5), **b** Hurricane intensity storms (cat 1–5), **c** major hurricanes (cat 3–5) and **d** very intense tropical cyclones (cat 4–5)

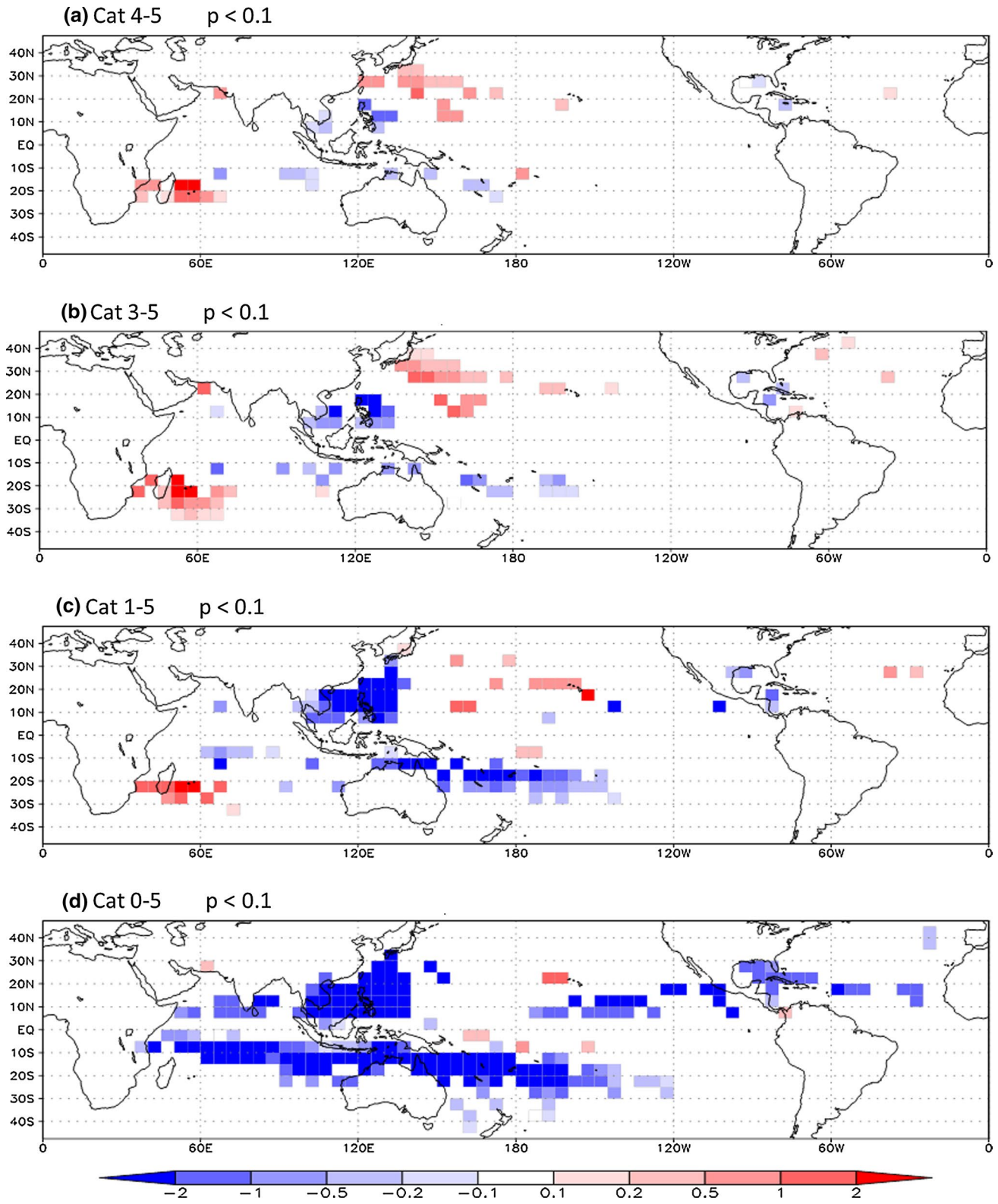

Fig. 5 Same as Fig. 4 but only the statistically significant areas, where *p* value is less than 0.1, are shown

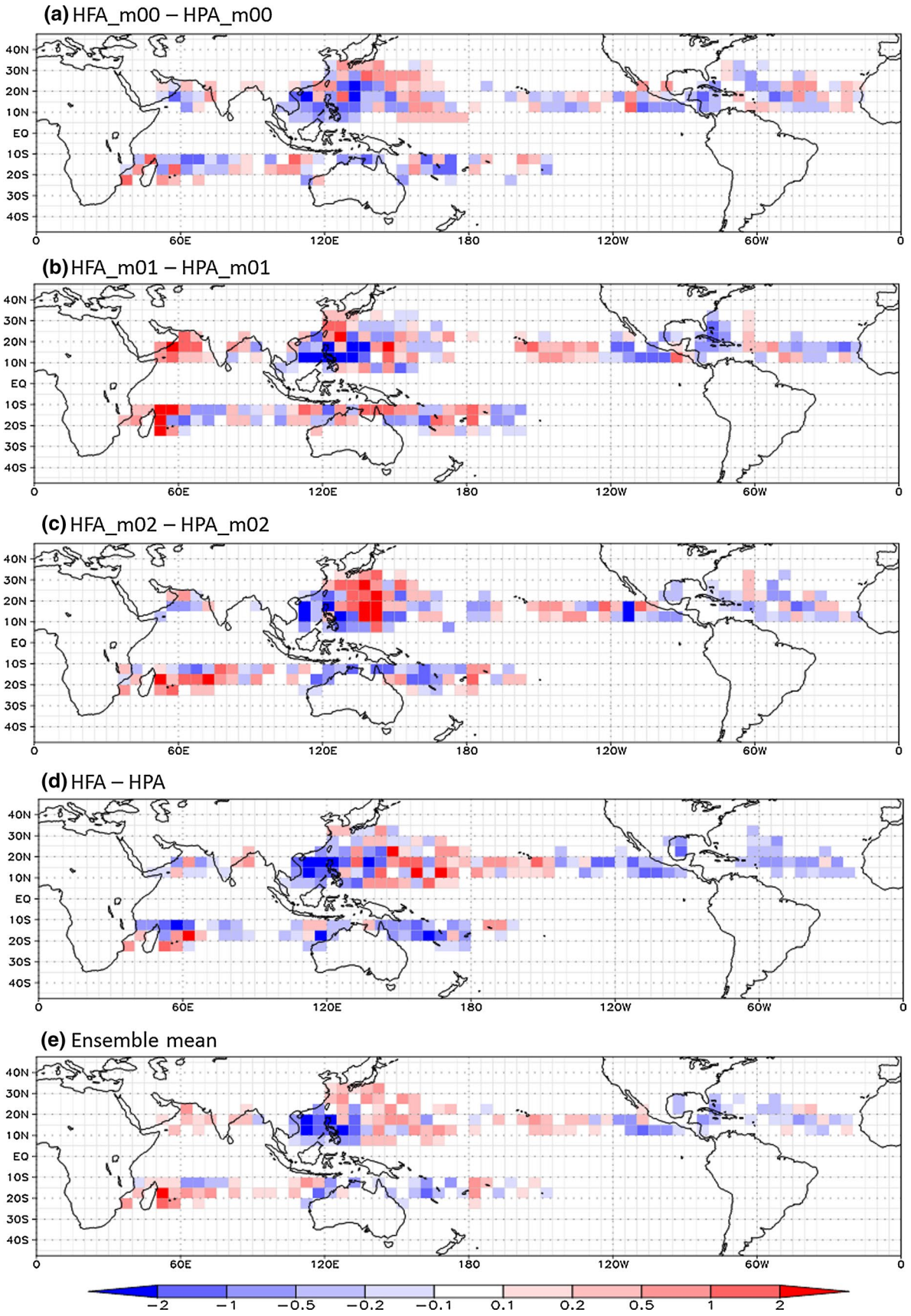
(a) HFA_m00 – HPA_m00
(b) HFA_m01 – HPA_m01
(c) HFA_m02 – HPA_m02
(d) HFA – HPA
(e) Ensemble mean
40N
30N
20N
10N
EQ
10S
20S
30S
40S
0
60E
120E
180
120W
60W
−2
−1
−0.5
−0.2
−0.1
0.1
0.2
0.5
1
2

◂**Fig. 6** Changes in occurrence frequency of very intense tropical cyclones (cat 4–5) of individual members of PD and GW simulations with the same model but different initial conditions. **a** F13 minus P4, **b** F14 minus P5, **c** F15 minus P6, **d** F16 minus P7, **e** ensemble mean of the four experiments [(**a**)–(**d**)]

Figure 3 shows the geographical distributions of the occurrence frequency (TC days) of very intense tropical cyclones (cat 4–5) in the observation, the ensemble means of PD and GW experiments and their difference. The TC days shown in Fig. 3 are TC days per decade in each 5° × 5° grid box. The geographical distribution of the TC days of the PD simulation (Fig. 3b) agrees well with that of observation (Fig. 3a), although we can see some differences in these distributions. We consider that some of these differences are rather expected because the PD simulation is an ensemble mean of the 11 members, while the observation is a single realization. As shown in Fig. 3d, the TC days of very intense tropical cyclones increase in most regions in the Northern Hemisphere except for southwestern part of the Northwest Pacific, the Northeast Pacific and westernmost part of the North Atlantic. In the Southern Hemisphere, the TC days decrease in most parts except for the western parts of the South Indian Ocean. Because the TC days decrease in some parts but increase in other parts of the Northwest Pacific Ocean or the Northeast Pacific Ocean, the changes are relatively small when averaged over these ocean basins (see Table 2). It is interesting to note that the pattern of the changes in TC days shown in Fig. 3d is similar to that shown in Knutson et al. (2015). The similarity between the two patterns, one obtained by statistical downscaling and the other obtained by dynamical downscaling, suggests that both the patterns are physically reasonable, irrespective of the downscaling methods. We also note that there are some notable differences between the two patterns, particularly in the eastern North Pacific. This difference is probably not due to the different downscaling methods but due to the difference in the changes in the number of all tropical storms (cat 0–5) simulated by the respective global models. Our results show 23.5 % decrease of all tropical storms in Northeast Pacific, while Knutson et al. (2015) show 16.3 % increase.

The geographical distributions of the changes in TC days in various intensity categories are shown in Fig. 4. The pattern of changes in TC days in cat 3–5 is similar to those of cat 4–5, but the areas of decreasing TC days expand a little. The patterns of changes in TC days in cat 1–5 and cat 0–5 is also similar to those of cat 4–5, but the areas of decreasing TC days further expand, and in cat 0–5 the areas of decreasing TC days dominate the entire globe except for the central North Pacific Ocean, south western part of the South Indian Ocean, northern part of Arabian Sea and northwestern part of the Bay of Bengal.

4 Discussion

4.1 Statistical significance

In the previous section, we have noted that the TC numbers or TC days of all tropical storms (cat 0–5) decrease globally and by ocean basins and these changes are statistically significant. On the other hand, the changes are not statistically significant for the tropical cyclones in more intense categories (Table 2). Figure 5 shows the geographical distribution of statistically significant changes in TC days in each intensity category. In Fig. 5, the p value is calculated for each 5° × 5° grid box using a two sided Mann–Whitney–Wilcoxon test, and a grid box is considered to be statistically significant if the p value is less than 0.1. We note that very small regions of the changes is statistically significant for the most intense category cat 4–5 (Fig. 5a). The areas of statistically significant changes increase for the less intense tropical cyclone categories (Fig. 5b–d). However, the changes are not statistically significant in many areas even for all tropical storms (cat 0–5). By comparing Fig. 4d and Fig. 5d, we note that the areas of increasing TC days of all tropical storms (cat 0–5) are not statistically significant.

According to a simple statistical significance test, only a small portion of the changes in very intense tropical cyclones (Fig. 4a) is statistically significant. However, this does not necessarily mean that the changes shown in Fig. 4a are not reliable at all. The pattern of the changes is systematic and robust among different intensity categories. This response could be physically reasonable but more simulations would be required to improve the simulated statistics.

4.2 Effect of ensemble average

An advantage of a statistical downscaling method is that it can use larger amount of data that is available from ensemble experiments. This enables us to estimate more reliable statistics than by a single experiment. Figure 6 shows the pattern of the changes in TC days of very intense tropical cyclones (cat 4–5) for four individual experiments (Fig. 6a–d) and ensemble mean of the four experiments (Fig. 6e). The four experiments are the same model simulations but only the initial conditions are different from each other. The pattern of estimated TC day changes by individual model is considerably noisy (Fig. 6a–d), indicating that the data sample size is too small to make a reliable estimate the changes at each grid box. The pattern of ensemble mean changes (Fig. 6e) is less noisy and resemble to the all member ensemble mean pattern shown in Fig. 4a, indicating that the four member ensemble mean estimate is more reliable than the individual model estimates.

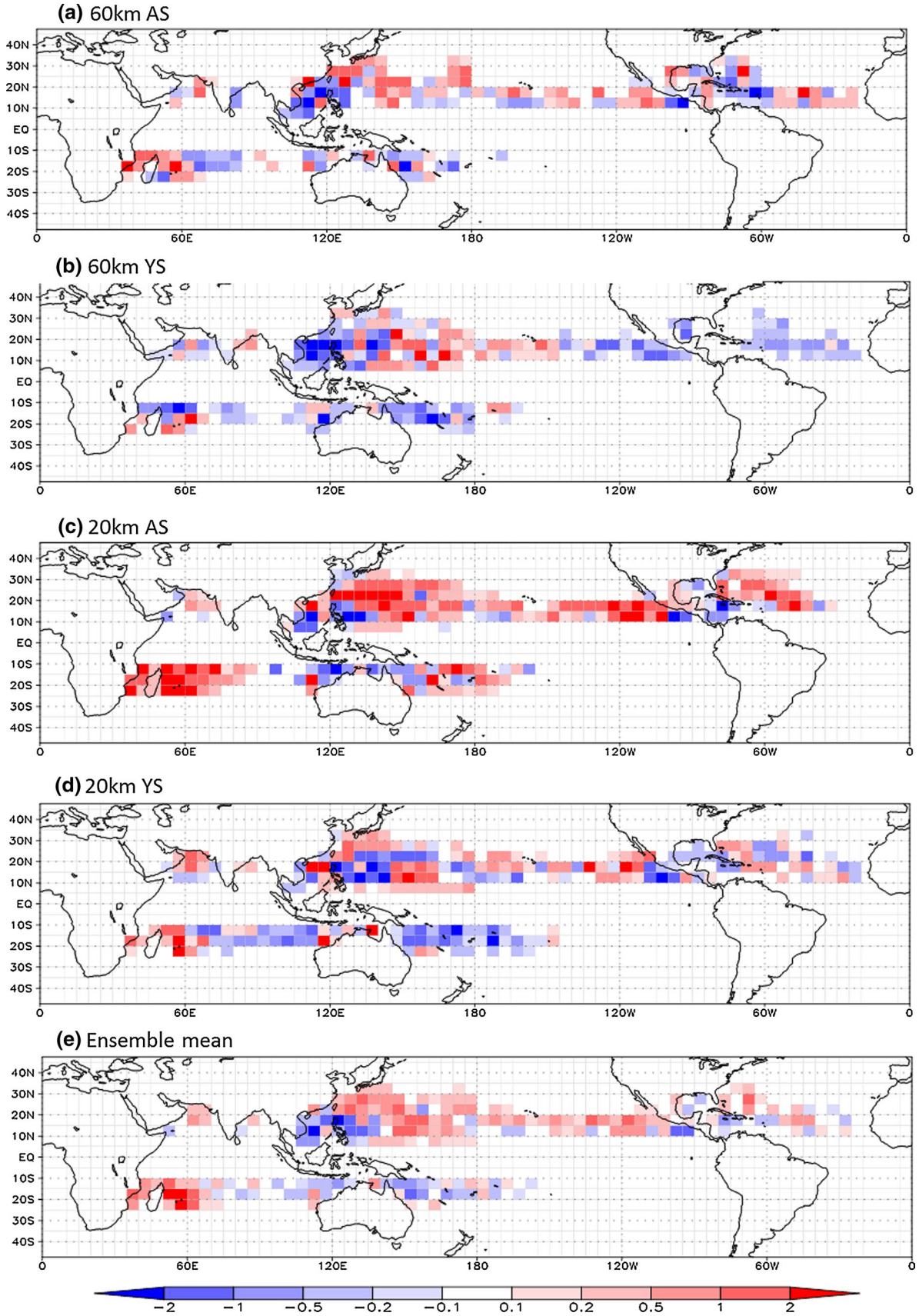
(a) 60km AS
(b) 60km YS
(c) 20km AS
(d) 20km YS
(e) Ensemble mean
40N
30N
20N
10N
EQ
10S
20S
30S
40S
0
60E
120E
180
120W
60W
−2
−1
−0.5
−0.2
−0.1
0.1
0.2
0.5
1
2

◂**Fig. 7** Same as Fig. 6 but for members of PD and GW simulations with different resolution (60 or 20 km) and different convection scheme (AS or YS). **a** F1 minus P1 [60 km AS], **b** F16 minus P7 [60 km YS], **c** F28 minus P10 [20 km AS], **d** F29 minus P11 [20 km YS], **e** ensemble mean of the four experiments [(**a**)–(**d**)]

It should be noted that our ensemble experiment is a multi-model ensemble experiment using models with different resolutions and different convection schemes. To illustrate the uncertainty due to models, the geographical patterns of the changes estimated by four different models and their ensemble mean are shown in Fig. 7. The four models are different from each other by resolution (20 or 60 km) and convection scheme (AS or YS). There are considerable differences among the changes estimated by individual experiments. Only the experiment with 60 km resolution and YS convection scheme (Fig. 7b) shows a decreasing TC day pattern over the Northeast Pacific and North Atlantic, but it is difficult to say that this is due to resolution or convection scheme or both. Comparing Fig. 7a (Fig. 7c) and Fig. 7b (Fig. 7d) indicates that YS convection scheme tend to show more decreasing TC day trend over the Northeast Pacific and North Atlantic. Similarly, comparing Fig. 7a (Fig. 7b) and Fig. 7c (Fig. 7d), lower resolution (60 km grid) models tend to show more decreasing TC day trend over these ocean basins.

4.3 Intensity bias correction

The method of statistical downscaling in the present study is based on an intensity bias correction. We applied the statistical bias correction for each 5° latitude band in the each ocean basin. An advantage of this method is that we can make bias corrections depending on the latitudes. It should be noted that this method cannot make bias correction depending on longitudes. A slow developing bias in a simulated westward moving tropical cyclone is likely to cause a westward intensity bias (more intense in the western part of the track). We note that over the South China Sea the simulated frequency of very intense tropical cyclones (Fig. 3b) is much larger than that of observation (Fig. 3a). This is probably due to the westward intensity bias, indicating that this bias is not corrected by our bias correction method.

An obvious limitation of the statistical bias correction method of the present study is that the statistical sample size is not sufficient at high latitudes or for very intense tropical cyclones. To make a more reliable bias correction, a much larger number of ensemble experiments may be necessary.

5 Conclusions

We have presented a projection of changes in the frequency of intense tropical cyclones in the future warmer climate estimated by a statistical downscaling of an ensemble of many high-resolution global model experiments. The experiments include 11 member 25 year present day (PD) climate simulations and 29 member 25 year future global warming (GW) climate simulations, using MRI-AGCM 3.1 or 3.2, with different initial conditions, different convection schemes (AS, KF or YS), different resolution (20 or 60 km) and different SST changes for GW climate simulations. The results indicate that the changes in the frequency (TC days) of the very intense tropical cyclones (category 4–5, $V_{max} \geq 59$ m/s) are not uniform on the globe. The frequency will increase in most regions but decrease in the south western part of Northwestern Pacific, the South Pacific, and eastern part of the South Indian Ocean. It is interesting to note that the pattern of the changes in TC days shown in Fig. 3d is similar to that shown in Knutson et al. (2015). The pattern of changes in the frequency of major hurricanes (category 3–5, $V_{max} \geq 50$ m/s) is similar to that of very intense tropical cyclones, with a little larger area of decreasing frequency. The patterns of changes in the frequency of less intense tropical cyclones (category 1–5, $V_{max} \geq 33$ m/s or cat 0–5, $V_{max} \geq 17$ m/s) are also similar to that of the intense tropical cyclones, but the area of decreasing frequency systematically expands for less intense tropical cyclones, and in cat 0–5 the areas of decreasing TC days dominate the entire globe.

According to a simple statistical significance test, only a small portion of the changes in very intense tropical cyclones is statistically significant (Fig. 5). However, as the pattern of the changes is very systematic and robust among different intensity categories (Fig. 4), the pattern could be physically reasonable. Moreover, we have noted that the pattern of the changes in very intense tropical cyclones shown in Fig. 3d is similar to the pattern shown in Knutson et al. (2015). The similarity of the two patterns suggests that both the patterns are physically reasonable. To make a more reliable, more statistically significant and more quantitative projection of the occurrence frequency of intense tropical cyclones, we need larger number of ensemble experiments, as well as an improvement in the method of statistical downscaling. These are important subjects of future work.

Acknowledgments This work was conducted under the framework of the Program for Risk Information on Climate Change (SOUSEI program) and Innovative Program of Climate Change Projection for the twenty first Century (KAKUSHIN Program) of the Ministry of Education, Culture, Sports, Science and Technology (MEXT) of Japan. Calculations were performed on the Earth Simulator of JAMSTEC.

References

Arakawa A, Schubert WH (1974) Interaction of cumulus cloud ensemble with the large-scale environment. Part I. J Atmos Sci 31:674–701

IPCC (2013) Climate change 2013: the physical science basis. Stocker TF et al (eds) Cambridge University Press, Cambridge

Kain JS, Fritsch JM (1990) A one-dimensional entraining/detraining plume model and its application in convective parameterization. J Atmos Sci 47:2784–2802

Kain JS, Fritsch JM (1993) Convective parameterization for mesoscale models: the Kain–Fritsch scheme. In: Emanuel KA, Raymond DJ (eds) The representation of cumulus convection in numerical models of the atmosphere. Meteorol Monogr Am Meteorol Soc 46:165–170

Knutson TR et al (2010) Tropical cyclones and climate change. Nat Geosci 3:157–163. doi:10.1038/ngeo779

Knutson TR et al (2013) Dynamical downscaling projections of twenty-first-century Atlantic hurricane activity: CMIP3 and CMIP5 model-based scenario. J Clim 26:6591–6617. doi:10.1175/JCLI-D-12-00539.1

Knutson TR, Sirutis JJ, Zhao M, Tuleya RE, Bender MO, Vecchi GA, Villarini G, Chavas D (2015) Global projections of intense tropical cyclone activity for the late twenty-first century from dynamical downscaling of CMIP5/RCP4.5 scenarios. J Clim 28:7203–7224. doi:10.1175/JCLI-D-15-0129.1

Murakami H, Mizuta R, Shindo E (2012a) Future changes in tropical cyclone activity projected by multi-physics and multi-SST ensemble experiments using the 60-km-mesh MRIAGCM. Clim Dyn 39:2569–2584. doi:10.1007/s00382-011-1223-x

Murakami H et al (2012b) Future changes in tropical cyclone activity projected by the new high-resolution MRI-AGCM. J Clim 25:3237–3260. doi:10.1175/JCLI-D-11-00415.1

Murakami H et al (2015) Simulation and prediction of category 4 and 5 hurricanes in the high-resolution GFDL HiFLOR coupled climate model. J Clim 28:9058–9079. doi:10.1175/JCLI-D-15-0216.s1

Randall D, Pan D-M (1993) Implementation of the Arakawa–Schubert cumulus parameterization with a prognostic closure. The representation of cumulus convection in numerical models. Meteorol Monogr Am Meteorol Soc 46:137–144

Roberts M et al (2015) Tropical cyclones in the UPSCALE ensemble of high-resolution global climate models. J Clim 28:574–596. doi:10.1175/JCLI-D-14-00131.1.s1

Rayner NA, Parker DE, Horton EB, Folland CK, Alexander LV, Rowell DP (2003) Global analyses of sea surface temperature, sea ice, and night marine air temperature since the late nineteenth century. J Geophys Res 108:4407. doi:10.1029/2002JD002670

Sugi M, Yoshimura J (2012) Decreasing trend of tropical cyclone frequency in 228-year high-resolution AGCM simulations. Geophys Res Lett 39:L19805. doi:10.1029/2012GL053360

Unisys (2012) Unisys weather hurricane tropical data. http://weather.unisys.com/hurricane/

Walsh K et al (2016) Tropical cyclones and climate change. WIRES Clim Change 7:65–89. doi:10.1002/wcc.371

Wehner M, Prabhat Reed KA, Stone D, Collins WD, Bacmeister J (2015) Resolution dependence of future tropical cyclone projections of CAM5.1 in the U. S. CLIVAR Hurricane Working Group idealized configurations. J Clim 28:3905–3924. doi:10.1175/JCLI-D-14-00311.1

Yoshimura H, Mizuta R, Murakami H (2015) A spectral cumulus parameterization scheme interpolating between two convective updrafts with semi-Lagrangian calculation of transport by compensatory subsidence. Mon Wea Rev 143:597–621. doi:10.1175/MWR-D-14-00068.1

Zhao M, Held IM (2010) An analysis of the effect of global warming on the intensity of Atlantic hurricanes using a GCM with statistical refinement. J Clim 23:6382–6393. doi:10.1175/2010JCLI3837.1